ELSEVIER

Journal of Neuroscience Methods 154 (2006) 102–108

JOURNAL OF NEUROSCIENCE METHODS

www.elsevier.com/locate/jneumeth

A device for the electrophysiological recording of peripheral nerves in response to stretch

Jianming Li, Riyi Shi *

Weldon School of Biomedical Engineering and Department of Basic Medical Sciences, School of Veterinary Medicine, Purdue University, West Lafayette, IN 47907, USA

Received 30 August 2005; received in revised form 26 November 2005; accepted 5 December 2005

Abstract

The functional consequences of nervous tissue subjected to mechanical loads are of vital importance in successful clinical outcomes and in tissue engineered applications. In this paper, we developed a new ex vivo device that permitted the recording of nerve action potentials while the nerve was subjected to elongation. Experimental results showed guinea pig nerves to possess an inherent tolerance to mild stretch. The mean elongation at which the compound action potential (CAP) amplitude began to decrease was found to be $8.3 \pm 0.56\%$. The CAP response to stretch was immediate beyond this threshold. After $17.5 \pm 0.74\%$ elongation, the CAP levels decreased to approximately 50% of its uninjured values. When allowed to relax, the CAP recovered almost completely within minutes. Based on the temporal scale of the CAP response and the presence of oxygen during testing, we conclude that the initial mechanism to CAP degradation cannot be ischemia. Since it is inherently difficult to study mechanical damage independent of hemodynamic factors in vivo, the developed model could be used to further elucidate the injury mechanisms of stretch-induced trauma. The design of the ex vivo chamber will also permit the administration and assessment of pharmacological agents on electrical conduction in various deformation conditions.

Keywords: Strain; Sciatic nerve; Grease gap recording; Compound action potential

1. Introduction

From a morphological perspective, peripheral nerves are naturally structured to withstand mild levels of stretch (Fig. 1A). The tortuous pattern of axonal elements and surrounding axolemma offer a protective mechanism against stretch injuries (Sunderland, 1990). Previously, there have been several studies attempting to define tensile loads that translate into measurable anatomical damage (Haftek, 1970; Rydevik et al., 1990; Sunderland, 1990; Spiegel et al., 1993; Ninan, 2003). However, it is reasonable to assume that functional damage may occur prior to any permanent morphological change. Using mostly in vivo models, later studies have aimed to characterize such conduction behavior during maintained levels of nerve stretch (Denny-Brown and Doherty, 1945; Kwan et al., 1992; Wall et al., 1992; Driscoll et al., 2002; Takai et al., 2002; Jou et al., 2000). Yet due to the confounding variables of in vivo models, it was difficult to determine the initial mode of injury. Indeed during nerve elongation, there is constriction of the vasculature and decreased blood flow within nervous tissue (Lundborg and Rydevik, 1973; Jou et al., 2000). The subsequent ischemia is sometimes believed to be the primary culprit leading to functional deficit, although some suggest there may be an earlier mechanism ascribed to mechanical deformation (Kwan et al., 1992; Ochs et al., 2000; Driscoll et al., 2002). We also hold the view that prior to ischemic injury there is a mode of mechanical injury that is responsible for the observed conduction block. However, reliable ex vivo models are still lacking. Thus, the present study attempts to elucidate the initial process of functional deficit through the development of an ex vivo measurement device. The implementation of our unique isolation chamber permits us to continuously measure compound action potentials (CAP) and collective cell membrane integrity while the nerve is subjected to stretch. This novel acute injury model also allows us to compare and contrast conduction block caused by tissue deformation to that of ischemic insult.

* Corresponding author. Tel.: +1 765 496 3018; fax: +1 765 494 7605.
E-mail address: riyi@purdue.edu (R. Shi).

0165-0270/$ – see front matter © 2005 Elsevier B.V. All rights reserved.
doi:10.1016/j.jneumeth.2005.12.007

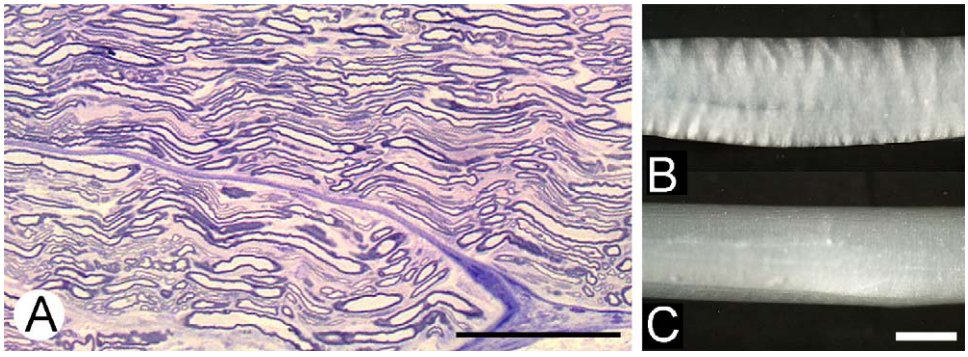

Fig. 1. (A) High magnification of guinea pig tibial nerve sectioned longitudinally. Samples were stained with toluidine blue as a marker for myelin. The histology reveals the natural wavy pattern typical of peripheral nerves. Bar: 100 μm. (B) Low magnification of guinea pig tibial nerve at rest (retracted) length. The vertical light and dark bands are an optical phenomena (bands of Fontana) caused by the microscopic undulations of the nerve architecture (A). (C) During stretch, the axonal undulations straighten and the vertical bands of Fontana disappear (Clarke and Bearn, 1972). Elongations at which these bands vanished were found to be $9.15 \pm 0.19\%$ ($n = 8$). These values are lower than the data reported by Pourmand, who observed the disappearance of the bands at 14% strain with rat sciatic nerves (Pourmand et al., 1994). Upon release of stretch the bands are restored as the nerve rebounds to initial length. Based on our observations, the disappearance of these bands may serve as an indicator for the onset of conduction block. Bar: 0.5 mm.

2. Materials and methods

2.1. Nerve isolation

All animals used in this study were handled in strict accordance with the National Institutes of Health guide for the Care and Use of Laboratory Animals. The experimental protocol was approved by the Purdue Animal Care and Usage Committee.

Adult female guinea pigs (ranging from 325 to 500 g) were anesthetized using ketamine (80 mg/kg) and xylazine (12 mg/kg) and perfused with 15 °C Kreb's solution. The sciatic nerve (~5 cm long) was then excised and allowed to retract in an oxygenated (95% O_2, 5% CO_2) Kreb's solution for 10 min. After 10 min, a pair of dye lines approximately 12 mm apart was made on the nerve. This 12 mm distance served as the retracted reference gauge length that was used for subsequent elongation calculations. After dye marking, the sciatic nerves were then split with a #12 scalpel blade to isolate the tibial and peroneal components. The nerves were re-incubated in the bubbling Kreb's solution for an additional hour to recover from the surgical process. The composition of Kreb's solution was as follows (mM units): 124 NaCl, 5 KCl, 1.2 KH_2PO_4, 1.3 $MgSO_4$, 2 $CaCl_2$, 20 glucose, 10 sodium ascorbate, and 26 $NaHCO_3$, equilibrated with 95% O_2, 5% CO_2 to produce a pH of 7.2–7.4.

2.2. Experimental chamber and setup

The current experimental apparatus is a modification of the double sucrose gap chamber first devised by Shi and Blight (1996). Briefly, an acrylic chamber 30 mm long was machined with five wells as shown in Fig. 2. The sucrose gaps from the original apparatus were substituted with grease insulator slots that separated the middle compartment from the end wells. Vacuum grease placed in these wells formed a leak proof barrier that separated the fluid reservoirs. Each end well was filled with isotonic (120 mM) potassium chloride, while the center reservoir contained Kreb's buffer solution. Excised nerves were placed in a 1 mm wide central channel that extended through the chamber. The nerve ends were fixed by a stationary and moveable clamp. The moveable clamp was attached to a rigid bar, which was in turn mounted to a digital force transducer (Mark 10). The force transducer was bolted to a motorized micromanipulator (Newport). A clear acrylic lid was set over the entire chamber to seal the setup (not shown) and a built in gas line was used to control the gaseous environment (Fig. 3). Two pairs of Ag/AgCl electrodes on opposite sides of the chamber served to stimulate and record the nerve tissue. The electrodes were not in direct contact with the nerves. All electrophysiology recordings were made using a bridge amplifier (Neurodata Instruments) and data analysis was performed with custom PC Labview software (National Instruments). Control trials with the experimental setup showed stable electrophysiology for over an hour (Fig. 4) and nerve

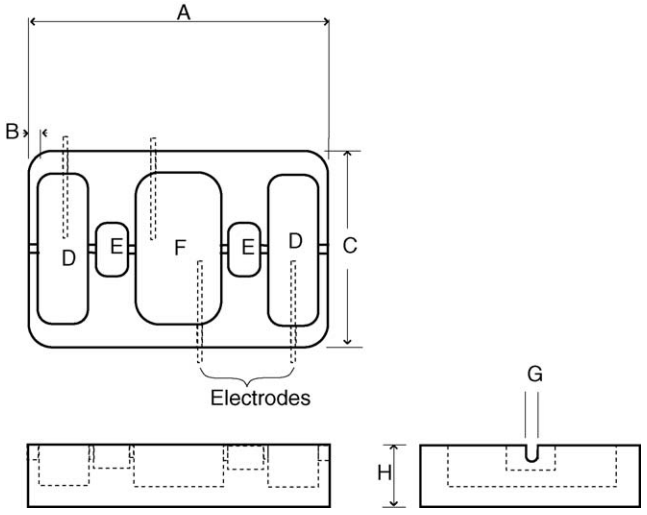

Fig. 2. Schematics of the acrylic isolation chamber that was modified from the version in Shi and Blight (1996). All dimensions given in millimeters. (A) 29, (B) 0.9 (typical), (C) 20, (D) 3.5 × 16.5 × 3 (length × width × depth), (E) 3.5 × 6 × 3, (F) 9.6 × 16.5 × 3.5, and (G) 1.0 DIA, 2 deep. The cover (not shown) was placed over the chamber and sealed with vacuum grease (Dow). The chamber is airtight except at the notches where the nerve exits the chamber. The covered chamber was found to keep oxygen tension at 26 ppm when measured with an oxygen sensor (WPI Inc.).

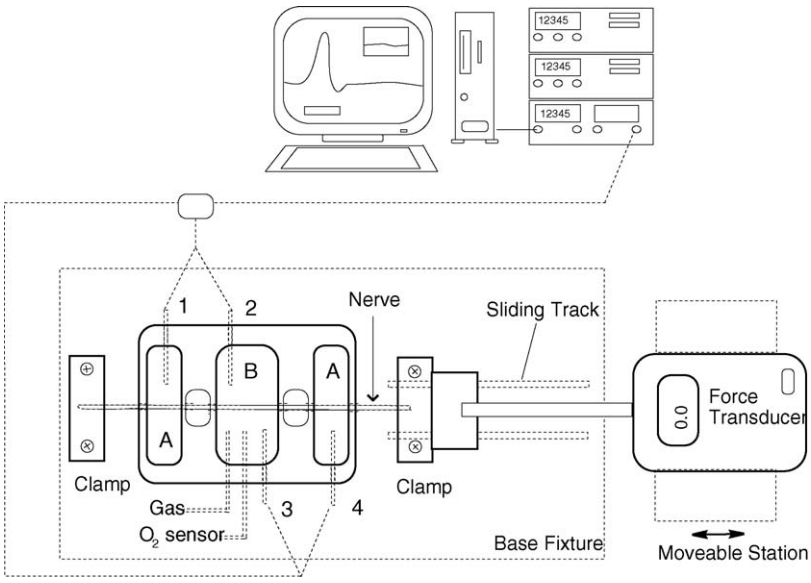

Fig. 3. Depiction of the three well isolation chamber and experimental setup. *Designations*: (1 and 2) recording electrode pair and (3 and 4) stimulating electrode pair; (A) isotonic (120 mM) potassium chloride and (B) Kreb's solution. The dotted line denotes the isolated nerve specimen. A drop of cyanoacrylate glue was placed on the nerve, which was then sandwiched between texturized rubber clamp pads. The left end clamp was fixed to the base platform while the right side clamp was attached to a rigid bar linked to a digital force transducer (Mark 10). The force transducer was bolted to a motorized micromanipulator (Newport Industries), which controlled clamp displacement. Electrode recordings were made with a Neurodata recorder. Stimulation was achieved with a Grass stimulator set at supramaximal intensity. Nerves were stimulated and recorded at 3 s time intervals.

viability for at least 3 h. Electrophysiology entailed the measurement of compound action potentials and compound resting membrane potential (gap potential). The gap potential is a quantity that relates to whole-nerve ionic permeability and serves as an indicator of membrane integrity (Shi et al., 2000).

2.3. Electrophysiological recording during stretch

2.3.1. Group A

After the 1 h incubation period, the peroneal/tibial nerve was randomly placed (distal left, proximal right or vice versa) into the isolation chamber. The resting nerve was then fixed to the stationary and moveable clamp. Next, viscous silicone vacuum grease (Dow Corning) was placed into the machined grease wells. Kreb's solution and isotonic potassium chloride was pippetted into appropriate wells. The clamp crosshead was then translated such that the dye marks on the nerve corresponded to the retracted gauge length. The cover was then placed over the chamber. A 95% O_2/5% CO_2 gas mixture was flowed into the gas line to aerate the nerve. Electrophysiology then commenced. While performing electrophysiology, the micromanipulator was activated, elongating the nerve at speeds ranging from 0.072 to 0.11 mm/s. When the real-time CAP magnitude decreased to approximately 50% of the initial value, the clamp was paused for 2.5 min and the micromanipulator displacement noted. After the 2.5 min hold, the crosshead was returned to its starting position at a rate same to the elongation speed. Nerve elongation was calculated as $(l - l_0)/l_0$, where l was the extended clamp-to-clamp nerve length and l_0 was the initial clamp-to-clamp nerve length. The nerve was maintained at temperatures in the range of 22–25 °C. Stimulation and recording was performed at a frequency of 0.33 Hz. All nerve samples were tested once and then discarded.

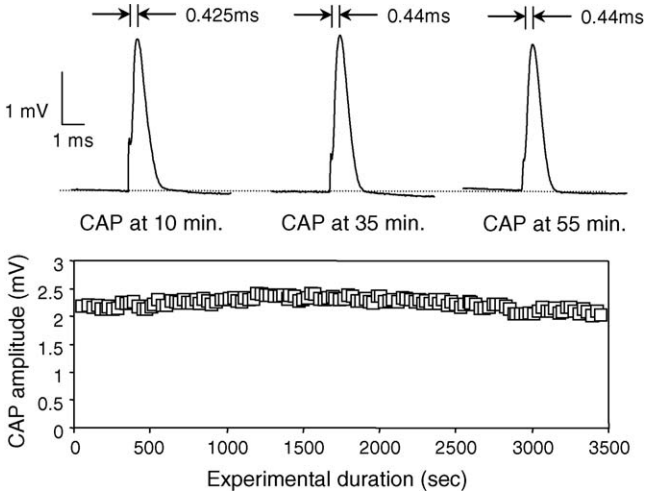

Fig. 4. Viability experiments demonstrate stable CAP values over a timeframe approaching 1 h. Instantaneous CAP waveforms with corresponding latency information at time intervals of 10, 35 and 55 min are also shown. Longer experiments proved that the nerves were viable for over 3 h using this apparatus.

2.3.2. Group B

To eliminate the possibility that Group A results were caused by artificial means from either methodology or apparatus, we performed a series of pre-stretch tests ($n = 6$) where the elongated state was considered the initial recording condition. Briefly, the nerve specimens were first loaded into the testing chamber and stretched to 20% of its retracted length. Silicone grease, ionic fluids, and a 95% O_2/5% CO_2 gas mixture were applied as previously described. At the 20% elongated state, the nerve

was stimulated (0.33 Hz) and the CAP recorded. After 5 min, the nerve was permitted to relax back to its retracted length at a crosshead speed of 0.119 mm/s. Concurrently, the electrophysiology was continuously reported during this retraction event.

2.4. Oxygen and glucose deprivation

2.4.1. Group C

To compare and contrast the nature of ischemic injury versus mechanical damage, ischemic tests were carried out using the same apparatus as the tension-electrophysiology recordings. As described, nerves were excised and placed into the isolation chamber. The nerve was fixed via the clamps and the clamp crosshead moved to correspond to the retracted nerve length. All necessary fluids and grease were applied. The chamber cover was set over the setup to control the local gaseous environment. A gas inlet tube was then inserted into the gas feed where a 95% O_2/5% CO_2 gas mixture was then flowed into the chamber for 10 min. Electrophysiology then commenced. Following a 10 min measurement phase, the oxygen mixture was substituted with a 95% N_2/5% CO_2 mix while the Krebs solution was exchanged with glucose-free Krebs (to simulate ischemic conditions). When the real-time CAP reached approximately 50% of its starting value, the nitrogen was exchanged with the original oxygen mixture and the glucose-free Krebs replaced with glucose Krebs. An oxygen sensor (WPI Inc.) was present in the Krebs chamber throughout the entire experiment to monitor dissolved oxygen content. The 95% N_2/5% CO_2 exposed Kreb's solution also produced a pH in the range of 7.2–7.4.

All the data presented are in the form of the mean ± standard error.

3. Results

3.1. Group A

When the nerve was elongated longitudinally from its retracted state, there was no immediate change in the CAP. As crosshead displacement further increased, however, a steady decrease in the CAP amplitude was seen (Fig. 5A). Trials using crosshead speeds in the range of 0.0718–0.11 mm/s showed similar characteristics. The threshold elongation at which the CAP began to decrease (consistent downward deflection in CAP history slope) was found to be 8.3 ± 0.56% ($n = 12$). The elongation corresponding to a 50% drop in the CAP was 17.5 ± 0.74% ($n = 11$). During the period when the nerve was held stretched (2.5 min), there was a slight recovery in the CAP. Measured latency during stretch was 2.0 ± 0.38 times longer when compared to unstretched values. After the hold phase, the nerve exhibited a recovery in the CAP after relaxation back to original length (Fig. 5A). Recovery gradually approached the starting steady-state amplitudes, although not fully in some cases (92.8 ± 2.9%). In conjunction with a recovery in the CAP, the latency also responded to tension removal, although they were still 26 ± 12% longer than initial uninjured values even after 20 min of recovery. Measurements of the gap potential during the initial, sustained stretch and recovery regions did not exhibit noticeable fluctuations (Fig. 5B).

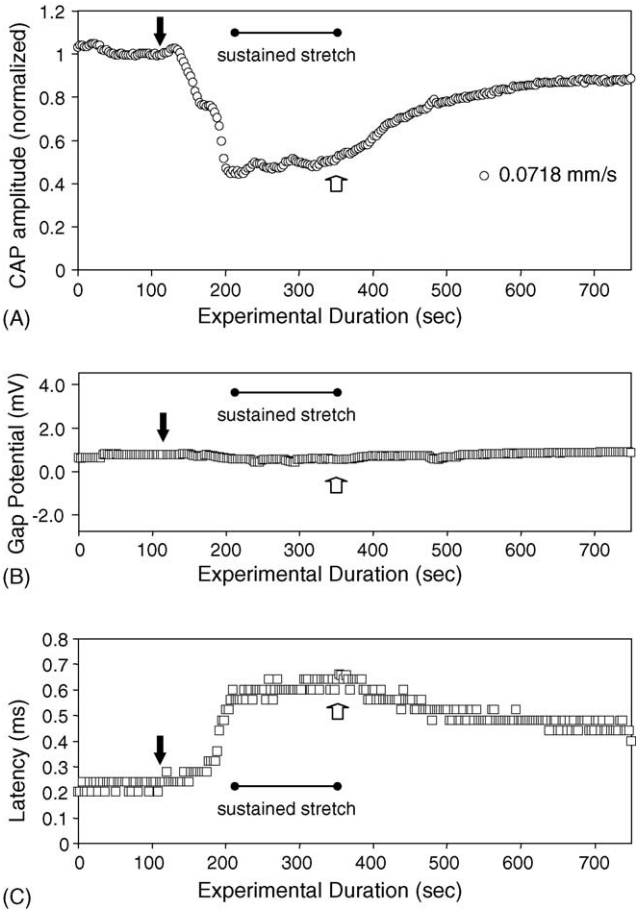

Fig. 5. (A) Representative sample plot of CAP amplitude as a function of time (crosshead speed of 0.0718 mm/s). Filled arrow indicates the start of stretch while the open arrow denotes end of stretch (also applies to (B and C)). The sustained stretch phase (no crosshead movement) is also shown. Note the time of stretch onset and the point where the CAP magnitude actually diminishes. The mean elongation at which the CAP amplitude began to decrease was at 8.3 ± 0.56 and 17.5 ± 0.74%, the CAP peak dropped by 50%. The CAP amplitude recovered to near starting values (92.8 ± 2.9%) 5–10 min post-stretch. (B) Gap potential recording corresponding to the above 0.0718 mm/s stretch test. The peaks represent event markers where stretch began and the initiation of the return phase. Note the near constant gap potential throughout the stretch and recovery regions. Marked changes in gap potential would generally signify a compromised membrane or dysfunctional ion pumps. (C) Simultaneous latency plot for the above 0.0718 mm/s stretch test. Note the increase in latency as elongation increases as well as its recovery (although incomplete). It was generally observed that latency was slower to recover than CAP values.

3.2. Group B

To elucidate whether the observed CAP response in Group A was caused by nerve deformation or by translational disturbances, we performed a series of trials in which the nerve was pre-stretched, placed in the chamber and then permitted to retract. Since the retraction process also creates translational motion, our objective was to investigate whether such movement diminished the CAP response. Our data suggest that translational perturbations of the nerve within the chamber does not explain

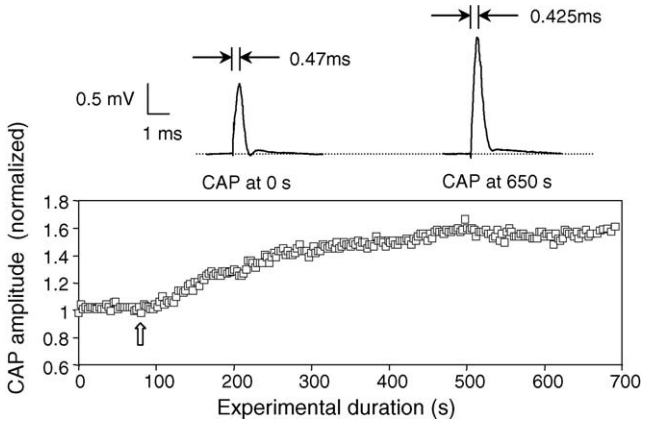

Fig. 6. A representative pre-stretch trial where the nerve was elongated to 20% and then allowed to retract at a rate of 0.119 mm/s back to original length. The ordinate values are normalized with respect to the initial (20% elongated) starting value. Open arrow denotes start of the retraction step.

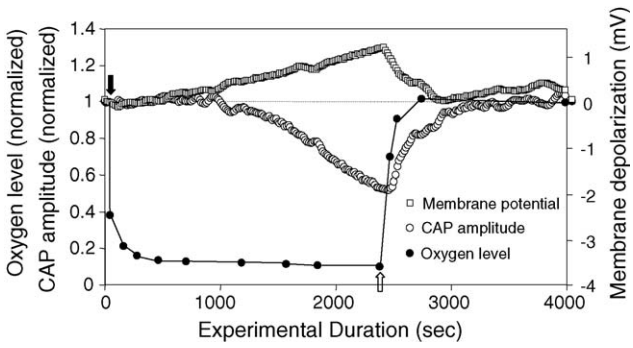

Fig. 7. Typical plots depicting simultaneous CAP amplitudes, gap potential and dissolved oxygen content. A near anoxic situation was created quickly after the application of 95% N_2/5% CO_2 gas (filled arrow event marker). The gradual and steady decrease in the CAP during the anoxic period highlights the delayed nature of ischemic injury. In conjunction with decreased oxygen tension, the gap potential also depolarized. Reintroduction of oxygen and glucose (open arrow event marker) quickly restored the CAP and gap potential. The CAP and oxygen plots were normalized with respect to initial steady-state conditions. Initial oxygen concentration: 26 ppm. Oxygen concentration during hypoxic phase: 2.5 ppm.

the results from Group A. Pre-stretch observations demonstrate a direct relationship between elongation and CAP amplitude as well as the ability of the nerve to recover from induced trauma. These results are further corroborated with pilot studies in which translational motion (3–7 mm) of the nerve did not significantly change the CAP response (data not shown).

We noted that when permitted to relax, the CAP magnitude increased by a factor of 1.75 ± 0.18 ($n = 6$) times the initial 20% stretch values (Fig. 6). Qualitatively and quantitatively, the pre-stretch plots compare favorably to the recovery phase data in Group A (Fig. 5A). No prominent change in gap potential was observed during the stretch and recovery phases. Similar to Group A trials, the latency generally decreased once the nerve was allowed to return to initial length.

3.3. Group C

At the outset of the ischemic tests, the CAP and gap potential were stable. After the superfusion of glucose-free Kreb's and substitution with nitrogen, the CAP remained steady for approximately 10–15 min, but then gradually diminished. Within 30 min, the CAP had decreased by 50%. The gap potential showed monotonic depolarization throughout this hypoxic phase. Reintroduction of glucose Kreb's and oxygen caused a quick repolarization in the gap potential. The repolarization event coincided with the complete recovery of the action potential magnitudes (Fig. 7). Latency values did not show prominent changes throughout the testing conditions (data not shown).

4. Discussion

Characterizing the response of peripheral nervous tissue to stretch is an important area of research that has clinical implications. Studying stretch insult requires accurate and reproducible models of injury. Previously, this was accomplished with mostly in vivo preparations (Haftek, 1970; Spiegel et al., 1993; Kwan et al., 1992; Wall et al., 1992; Theophilidis and Kiartzis, 1996; Jou et al., 2000; Driscoll et al., 2002; Takai et al., 2002). While data reported by these experiments have given insight into possible damage thresholds resulting in conduction or tissue damage, in vivo injury models incur some limitations that may be problematic. For example, in addition to mechanical deformation, a decrease in blood flow also occurs during stretch (Lundborg and Rydevik, 1973; Jou et al., 2000). This inhibition of the intraneural vasculature has been hypothesized to contribute to a decrease in measured CAP and conduction velocities. Investigating mechanical insult independent of ischemia is therefore challenging in vivo, due to coupling effects. Ochs et al. (2000) circumvented this problem with an in vitro stretch regime (rat sciatic and dog peroneal nerves) where the CAP was measured under controlled oxygen situations. However, their data showed considerable variability with some specimens showing a CAP amplitude rise, while others decreased with applied tension. But in specimens treated with collagenase, there was clear evidence that the CAP decreased with elevated strain levels (Ochs et al., 2000).

In our current study, we were similarly interested in the response of nerves to stretch and whether stretch-induced injuries were mediated by mechanical damage, ischemia or both. This question was addressed via the fabrication of a novel recording chamber. We should note that our setup differs from that of Ochs et al. (2000) in that with our apparatus, the nerve is not required to contact the electrodes. We believe a non-contact configuration to be an improvement since poor interfacing between the nerve and electrode may lead to recording inaccuracies. Secondly, the present apparatus is also capable of measuring membrane potential changes while the previous in vitro scheme could not (Ochs et al., 2000).

The results presented elucidate the non-ischemic mechanism of mechanical injury. The response of the nerves to elongation did not occur following initial clamp movement, but much later as the stretch magnitude increased to 8.3%. This confirms the obvious conclusion that during normal physiologic movements, the nerve functions uninhibited. Beyond the injury threshold, however, the CAP response became immediate. The observation

of a rapid electrophysiological response during traumatic injury is consistent with the results of Ochs et al. (2000). However, unlike their findings, the level of conduction block seen here is consistently proportional to the magnitude of imposed stretch. What is noteworthy is that the 8.3% elongation threshold corresponds very closely to the disappearance of the bands of Fontana, which we measured to occur at $9.15 \pm 0.19\%$ elongations ($n = 8$, Fig. 1B). This finding may be useful since it suggests the disappearance of the bands of Fontana could serve as an indicator for the onset of acute mechanical conduction block. We do not believe the drop in CAP magnitudes was produced by translational motion of the nerve. Although significant movement (i.e. beyond 7 mm) could interrupt the grease seals and reduce the quality of recorded signals, we did not find this to be a problem in the reported paradigm. Pre-stretch trials (Group B), in addition to the delayed onset of the CAP drop (Group A), clearly indicate elongation is most likely responsible for the CAP outcome and not nerve motion. There was no indication the CAP exceeded pre-injury levels during stretch as reported by Ochs et al. (2000). Such discrepancies could arise due to experimental apparatus or species differences. We should reiterate that our chamber is less sensitive to recording errors associated with inadequate nerve–electrode contact, a factor that could explain the large variations in the prior study (Ochs et al., 2000).

In the current experiments, we used a 50% drop in CAP as the maximum injury limit. This ceiling is somewhat arbitrary, but Jou et al. (2000) also suggested a 50% damage threshold based on their elongation studies. Our data revealed that a 50% drop in CAP occurred at a mean elongation of $17.5 \pm 0.74\%$. Latencies were approximately doubled for this elongation level as well. However, the compound membrane potential did not show measurable fluctuations. This information is noteworthy because it demonstrates that stretch is capable of eliciting severe drops in CAP do not cause significant membrane damage. The preservation of the membrane at these stretch amplitudes may explain the near reversible ($92.8 \pm 11.1\%$ recovery) nature of the injury. In contrast, latency times were consistently longer after stretch injury ($26 \pm 12\%$) and tended to recover more slowly than action potential amplitudes.

Tests with oxygen and glucose deprived preparations underscore the difference between ischemia and mechanical deformation injury. Severe hypoxic conditions require about 25–30 min for a 50% reduction in the CAP ($n = 7$, Fig. 7). In contrast, mechanical damage was immediate after exceeding the stretch threshold (i.e. 8.3%). Additionally, ischemic damage caused marked membrane depolarization, a feature not seen for our tested stretch magnitudes. It is presumed that the inhibition of membrane channel pumps contributes to the depolarizing phenomena (Peasley and Shi, 2002). Based on our results, many in vivo studies can be reinterpreted as a combination of mechanical and ischemic damage. We hypothesize the sequence of damage to be mechanical initially, followed by progressive ischemia. At higher elongations, rupture of Schwann tubes, myelin and connective tissue components may occur (Denny-Brown and Doherty, 1945; Haftek, 1970; Sunderland, 1978; Rydevik et al., 1990; Spiegel et al., 1993; Sunderland, 1990). This concept of mechanical damage followed by ischemic injury is important. Any therapeutic treatment designed to relieve stretch related dysfunction may need to address mechanical injury and ischemia as well.

The slow strain rates used was primarily due to limitations of the micromanipulator. However, future modifications would allow for faster strain rate testing, a condition that would better emulate rapid injury situations. Also, the recovery response of stretched nerves still warrants further investigation. Of key significance are values of elongation that may elicit irreversible functional damage or membrane disruption.

In conclusion, the development of appropriate models capable of deconvoluting confounding variables is critical in the understanding and treatment of mechanical insult on nerve tissue. We have thus presented a new technique capable of studying ex vivo tissue preparations under controlled loading situations. Using whole-nerve tissue has some unique advantages including the preservation of the natural three-dimensional matrix surrounding the axons. This cannot be said with comparable in vitro cellular assays (Galbraith et al., 1993; Smith et al., 1999). Furthermore, the current design of our isolation chamber may even allow one to study other forms of injuries such as combination traumatic situations (i.e. crush followed by tension) as well as the administration of pharmaceutical agents in their amelioration of conduction block (Jensen and Shi, 2003).

Acknowledgements

This research was funded by the NSF Integrative Graduate Education and Research Training (IGERT) Program in Therapeutic and Diagnostic Devices DGE-99-72770. We would also like to thank Phyllis Zickmund and Jennifer McBride for their assistance with the tissue preparation.

References

Clarke E, Bearn JG. The spiral nerve bands of Fontana. Brain 1972;95(1):1–20.

Denny-Brown D, Doherty MM. Effects of transient stretching of peripheral nerve. Arch Neurol Psychiat 1945;54:116–29.

Driscoll PJ, Glasby MA, Lawson GM. An in vivo study of peripheral nerves in continuity: biomechanical and physiological responses to elongation. J Orthop Res 2002;20(2):370–5.

Galbraith JA, Thibault LE, Matteson DR. Mechanical and electrical responses of the squid giant axon to simple elongation. J Biomech Eng 1993;115(1):13–22.

Haftek J. Stretch injury of peripheral nerve. Acute effects of stretching on rabbit nerve. J Bone Joint Surg Br 1970;52(2):354–65.

Jensen JM, Shi R. Effects of 4-aminopyridine on stretched mammalian spinal cord: the role of potassium channels in axonal conduction. J Neurophysiol 2003;90(4):2334–40.

Jou IM, Lai KA, Shen CL, Yamano Y. Changes in conduction, blood flow, histology, and neurological status following acute nerve-stretch injury induced by femoral lengthening. J Orthop Res 2000;18(1):149–55.

Kwan MK, Wall EJ, Massie J, Garfin SR. Strain, stress and stretch of peripheral nerve. Rabbit experiments ex vivo and in vivo. Acta Orthop Scand 1992;63(3):267–72.

Lundborg G, Rydevik B. Effects of stretching the tibial nerve of the rabbit: a preliminary study of the intraneural circulation and the barrier function of the perineurium. J Bone Joint Surg 1973;55B:390–401.

Ninan L. Study of nerve failure and the repair of nerves using synthetic and biological polymers. PhD Thesis. Purdue University; 2003.

Ochs S, Pourmand R, Si K, Friedman RN. Stretch of mammalian nerve ex vivo: effect on compound action potentials. J Peripher Nerv Syst 2000;5(4):227–35.

Peasley MA, Shi R. Resistance of isolated mammalian spinal cord white matter to oxygen-glucose deprivation. Am J Physiol Cell Physiol 2002;283(3):C980–9.

Pourmand R, Ochs S, Jersild Jr RA. The relation of the beading of myelinated nerve fibers to the bands of Fontana. Neuroscience 1994;61(2):373–80.

Rydevik BL, Kwan MK, Myers RR, Brown RA, Triggs KJ, Woo SL, Garfin SR. An ex vivo mechanical and histological study of acute stretching on rabbit tibial nerve. J Orthop Res 1990;8(5):694–701.

Shi R, Blight AR. Compression injury of mammalian spinal cord in vitro and the dynamics of action potential conduction failure. J Neurophysiol 1996;76(3):1572–80.

Shi R, Asano T, Vining NC, Blight AR. Control of membrane sealing in injured mammalian spinal cord axons. J Neurophysiol 2000;84: 1763–9.

Smith DH, Wolf JA, Lusardi TA, Lee VM, Meaney DF. High tolerance and delayed elastic response of cultured axons to dynamic stretch injury. J Neurosci 1999;19(11):4263.

Spiegel DA, Seaber AV, Chen LE, Urbaniak JR. Recovery following stretch injury to the sciatic nerve of the rat: an in vivo study. J Reconstr Microsurg 1993;9(1):69–74.

Sunderland S. The anatomy and physiology of nerve injury. Muscle Nerve 1990;13(9):771–84.

Sunderland S. Nerves and nerve injuries. 2nd ed. Baltimore: Williams and Wilkins; 1978.

Takai S, Dohno H, Watanabe Y, Yoshino N, Ogura T, Hirasawa Y. In situ strain and stress of nerve conduction blocking in the brachial plexus. J Orthop Res 2002;20(6):1311–4.

Theophilidis G, Kiartzis K. Stretching of an isolated part of the sciatic nerve of the frog (*Rana rindibunda*) causes excitation of its sensory nerve fibres. Neurosci Lett 1996;215(2):99–102.

Wall EJ, Massie JB, Kwan MK, Rydevik BL, Myers RR, Garfin SR. Experimental stretch neuropathy. Changes in nerve conduction under tension. J Bone Joint Surg Br 1992;74(1):126–9.